Bogolyubov Kyiv Conference "Problems of Theoretical and Mathematical Physics" || 24-26 September 2024

Nonequilibrium protection effect and spatial localization of noise-induced fluctuations: gas flow scattering on partially penetrable obstacle

Sergey Lukyanets | Oleksandr Kliushnichenko

Institute of Physics, NAS of Ukraine, Kyiv, Ukraine

Introduction

The main problem considered here is how the obstacle embedded in a gas flow can organize self-protection, by means of surrounding gas, against the gas flow and fluctuations. We show that this is possible in the regime of the non-linear dynamical screening which is result of the nonequilibrium transition that is accompanied by the emergence dense gas phase ahead of the obstacle due to blockade effect in a gas, the emergence of local invariants (invariant behavior of obstacle state that becomes insensitive to the main system parameters), spatial localization of induced gas fluctuations near gas domain wall. As a result the domain wall in a gas, instead of obstacle, becomes the main scatterer of the flow and protects obstacle state against external driving noise and fluctuations. This can be associated with nonequilibrium protection effect. Considered effects are closely related with skin- and edge-correlation ones inherent to non-Hermitian systems. To demonstrate these phenomena, we resort to the limiting case of the two-component lattice gas in a narrow channel with ring geometry. To describe the nonlinear nonequilibrium steady-state gas structures and long-time gas fluctuations near them we use the local equilibrium approach and the mean-field approximation.

Resorting to the particular case of quasi-1D case of the driven lattice gas doped with static impurities in a narrow channel with ring topology [1], we show:

- This nonequilibrium transition is accompanied by the emergence of local invariant. The obstacle state behaves as local firs integral (adiabatic invariant), becomes insensitive to the changes of system parameters, and to the fluctuations in a gas, in particular to the external drive noise.
- This transition can be considered as one with creation of the pair of topological defect and anti-defect (kink and anti-kink), one of which (anti-) is pined by obstacle, with changes of the main scatter of gas flow from structural lattice defect (obstacle) to topological defect in a gas (boundary of dense phase).
- The protection effect of obstacle state against gas fluctuations manifest itself in the strong localization of fluctuations near defect (domain wall of dense gas phase) and in the total their suppression at anti-defect (obstacle).

Model

We consider the limiting case of two component driving lattice gas in narrow channel with ring geometry. One of the components is assumed to be static and describes impurity sites,those partially occupy channel sell with mean concentration U, which corresponds to partially penetrable impurity site (obstacle) in the quasi-one dimensional limit [1]. To describe the nonequilibrium transition for NESSs and gas fluctuations near them we use the combination of the local equilibrium approach and the mean-field approximation neglecting the fast processes and short-range correlations [2–4]. This enables to describe the gas kinetics for the long time scales in the form of the mean field Smoluchowski equation for mean gas concentration at lattice sites n_k

$$\partial_t n_k = f^g_k(\vec{n}) = \sum_{j=k\pm1} (\nu_{jk} n_j h_k - \nu_{kj} n_k h_j), \quad (1)$$

where $h_k = 1 - u_k - n_k$, and $U_k = U\delta_{k,0}$ is given distribution of impurity particles, the asymmetry of hopping rates for back-forward particle jumps $\nu_{k,k\pm1} = \nu(1\pm g)$ is caused by the external driving field g. The steady state solution n^s_k of this equation ($\partial_t n_k = 0$ or $\vec{f}^g(\vec{n}^s) = 0$) determines NESSs which undergo nonequilibrium transition with the formation of two-domain gas structure at certain critical system parameters ($\bar{n}_c$, g_c, U_c), here $\bar{n}$ is mean gas concentration. The transition phase diagram, and typical behavior of gas density distributions are shown on Figs.1 and 2. The gas density fluctuations δn_k near nonequilibrium steady states n^s_k is governed by the Langevin equation that, for small δn_k, takes the form

$$\partial_t \delta n_k = \sum_j \left[\nu_{jk} \left(h^s_k \delta n_j - n^s_j \delta n_k \right) - (k \leftrightarrow j) \right] + \delta \tilde{I}_k, \quad (2)$$

with correlation function of the Langevin source

$$\left\langle \delta \tilde{I}_k(t) \delta \tilde{I}_{k'}(t') \right\rangle \approx 2\delta(t-t') \sum_j \nu_{kj} n^s_k h^s_j (\delta_{kk'} - \delta_{jk'}). \quad (3)$$

The nonequilibrium transition with the formation of two-domain NESS gas structure is characterized by the series of specific local effects.

*kliushnychenko@iop.kiev.ua
*lukyan@iop.kiev.ua

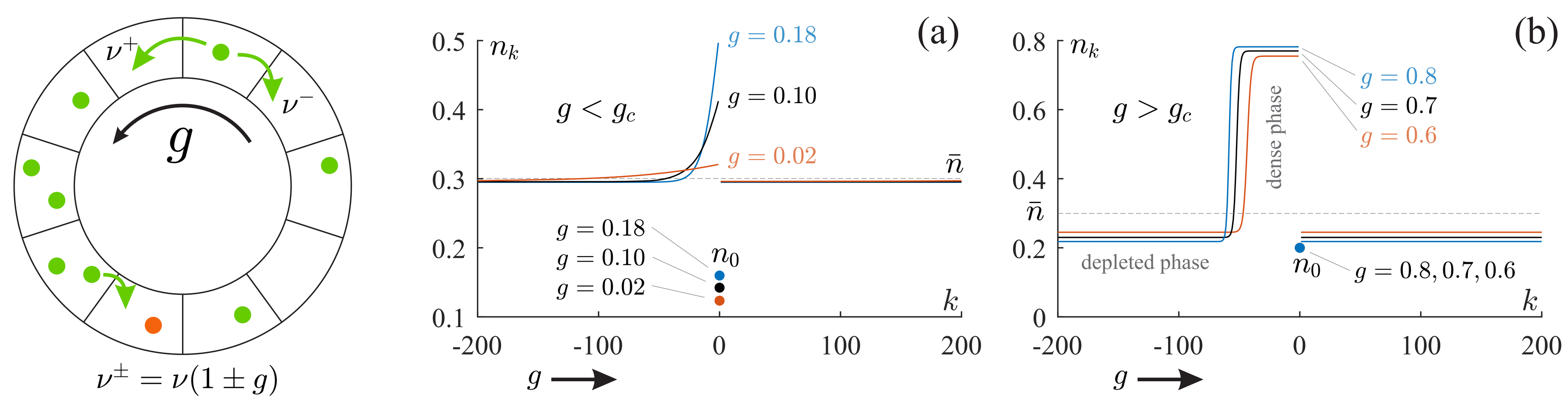

Figure 1: Periodic chain with ring topology and the impurity site (cell): $\nu^\pm = \nu(1 \pm g)$ are particle hopping rates along and against the direction of nonconservative field g. (a) Typical NESSs in subcritical regime, at $\bar{n} = 0.3$, $U = 0.6$, and $g = 0.02, 0.1, 0.18 < g_c$. (b) Typical NESSs in overcritical regime at $\bar{n} = 0.3$, $U = 0.6$, and $g = 0.6, 0.7, 0.8 > g_c$. The number of lattice sites $L_0 = 401$, the ring length $2L = 400\ell$, with lattice constant ℓ. The distributions in (a) and (b) were obtained from direct numerical solutions of the mean-field Eq. (1) as steady-state profiles established after $\approx 1.6 \times 10^7$ time steps of evolution since the driving field was switched from $g_0 = 0$ to g at $t_0 = 0$. The resulting NESS was regarded as finally established if $\max_k[n_k(\tau) - n_k(\tau - \Delta\tau)] \leq 10^{-30}$ with $\Delta\tau = 0.01$, where $\tau = \nu t$.

1. Emergence of Local Invariants

After the transition, the state of impurity site $n^s_0 = (1-U)/2$, site occupancy by gas particles, demonstrates invariant behavior, becomes insensitive to the farther changes of the main system driving parameters such as gas concentration $\bar{n}$ and external driving field g, Fig. 1. This local invariant behaves like the local first integral (for example, $(\vec{f}^g, \nabla_{\vec{n}}) n_0|_{\vec{n}^s(g')} \approx n^s_0$ at sudden switching of external field from g' to g), or as adiabatic invariant at least that was illustrated numerically, Fig. 2. This invariant describes the half-filling saturation of impurity site and serves as the local order parameter, on a par with integral ones, for this transition, see Fig. 2. For such local invariant, $n_0(g, \bar{n}) = \text{const}$, to exist is necessary strong correlated behavior or synchronization of the the impurity edge states at farther changes of g and/or $\bar{n}$, that is described by the second local invariant $n_{-1}(t) + n_1(t) = 1$. Thus, this transition is accompanied by the one from the skin to edge-correlation effect, see [5–7].

2. Nonequilibrium Protection Effect

As a result, the state of impurity site, $n^s_0 = (1-U)/2$, becomes insensitive to the gas fluctuations and the noise of the external driving field g, see Fig. 1 and 2. The nonequilibrium transition with the onset of two-domain gas structure can be considered as the creation of the pair of topological defects: the kink and anti-kink. These two topological defects in the gas correspond to two domain walls spatially limiting the dense gas phase. The first defect (kink) is "free" as it position is determined by the driving parameters as external field g, gas concentration $\bar{n}$. The anti-defect (anti-kink) is pinned by impurity site. Below the transition, the gas flow scatters on the structural lattice defect, i.e., impurity-site, that leads to the effect similar to the skin-effect [14–18]. After the transition, the flow scatters on free topological defect (kink) that protects own anti-defect from change of external condition, i.e., protects the state of impurity site. The nonequilibrium protection effect most pronouns manifests itself in the spatial localization of gas fluctuations.

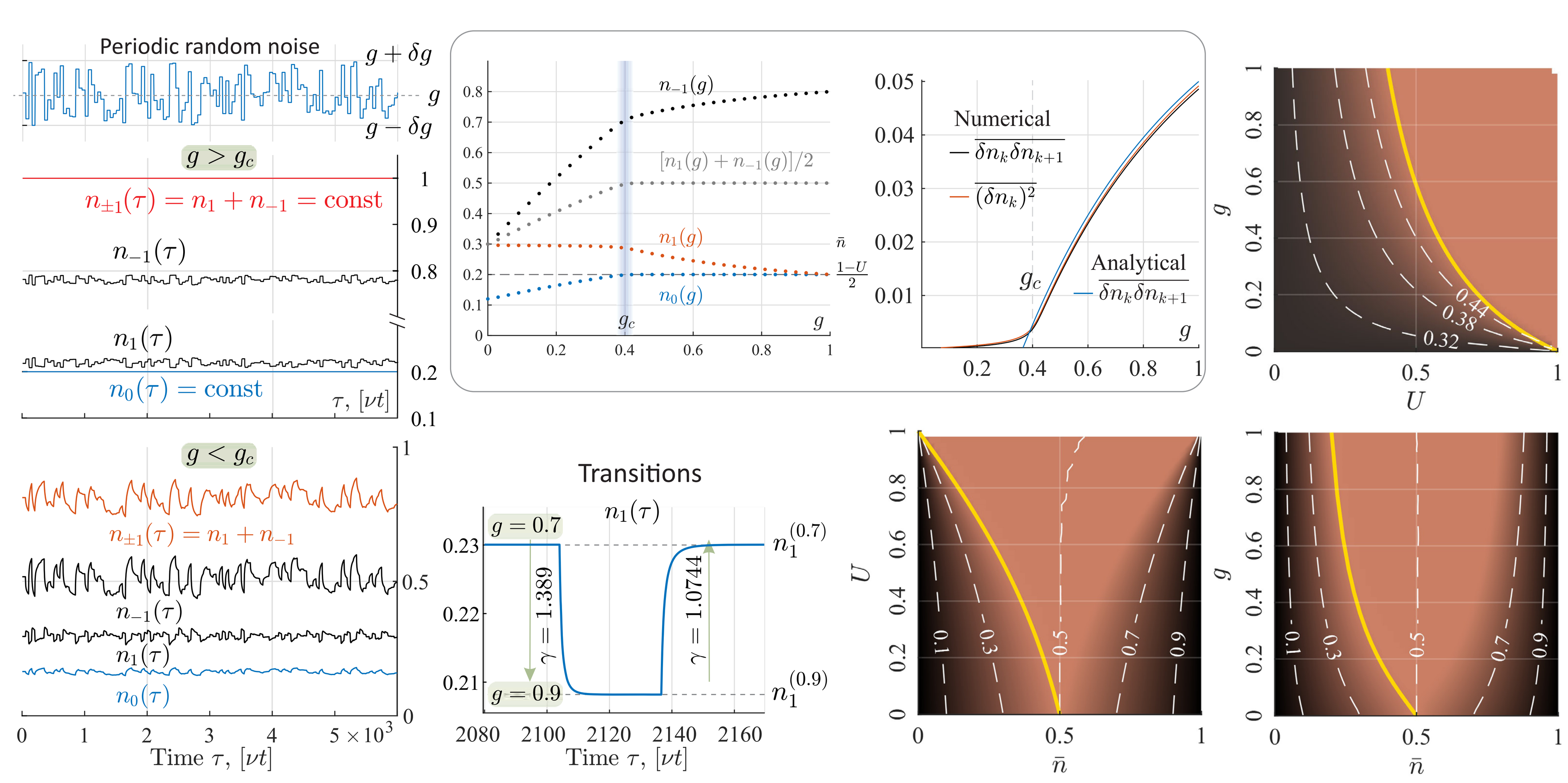

Figure 2: *Left:* Numerical illustration of the emergence of local invariants (local first integrals) $n_0(\tau) = (1-U)/2 = \text{const}$ and $n_{\pm1}(\tau) = n_1(\tau) + n_{-1}(\tau) \approx 1$ after nonequilibrium transition at $g > g_c$ for the case of driving field noise $g(\tau) = g + \delta g(\tau)$. Exploited noise sample is shown at the top panel and has switching frequency $\lambda = 0.02$. The drive $g(t)$ fluctuates around $g = 0.2$ (subcritical regime) or $g = 0.8$ (overcritical regime) with amplitude $|\delta g(t)| \leq 0.1$. Here, ring length $2L = 400\ell$, average density (filling fraction) $\bar{n} = 0.3$, and $U = 0.6$. Transition inset for $n_1(\tau)$ shows relaxation between $|g = 0.7\rangle \rightleftarrows |g = 0.9\rangle$ with dominant asymptotic behavior $\sim e^{-\gamma\tau}$, implying decay rate $\gamma \gg \lambda$. *Right:* Two-dimensional projections of the critical surface for the phase diagram given in $(U, \bar{n}, g)$ parameter space: (a) $(U, \bar{n})$-projection at $g = 0.5$, (b) (g, U)-projection at $\bar{n} = 0.3$, and (c) $(g, \bar{n})$-projection at $U = 0.6$. Analytically estimated phase boundaries (solid lines) are given by relation $U(\bar{n}) = 1 - [4\bar{n}(1-\bar{n})]/(3 - 4\bar{n})$. *Center inset*: (i) Occupations of impurity site n_0, its edges $n_{\pm1}$, and their half-sum as a function of external field g. (ii) Inter-particle correlations at the nearest sites $\overline{\delta n_k \delta n_{k+1}}$, where $\delta n_k = n_k - \bar{n}$, and $\overline{(\dots)} = L_0^{-1} \sum_k (\dots)$. Here, $\bar{n} = 0.3$, $U = 0.6$, and $L_0 = 401$.

Model notes

In contrast to the most Asymmetrical Simple Exclusion Processes (ASEP) models on a ring resulting in the blockade effect in a gas caused by an obstacle [8–9], where obstacles often realized via defect bonds, so called slow bonds [10–13], as locally reduced inter-site transition rates or as reduced inter-site exchange rate between particles of different sorts, we implement the obstacle by means static impurity particles as the partially transparent impurity-site that corresponds to the narrow channel cell partially occupied by impurity (heavy component) gas particles with concentration U. This leads not only to the decreasing of the occupation probability of impurity-site by gas particles (due to the decreasing of possible vacancies, $1 - U$), but also to the reducing of the transition rates of particles to this site from nearest neighbor ones. Qualitatively, U can be associated with the effective repulsion potential created by impurity atoms located in the channel cell. Another difference is to consider ASEP induced by an external driving field. As a result, the nonequilibrium transition to the blockade regime occurs not only at certain critical values of mean gas concentration and obstacle transparency parameters, but also critically depends on the driving field value g.

3. Spatial localization of induced fluctuations

To demonstrate this effect we resort to the particular case of a low-frequency noise $\delta g(t)$ of the external driving field $g(t) = g + \delta g(t)$, using the telegraph-like processes. We consider noise-induced gas density fluctuations $\delta n_k(t)$ near NESS n^g corresponding to the field g, Fig. 3. **In the subcritical regime ($g < g_c$)**, the gas fluctuations δn_k weakly concentrated near impurity site, structural lattice defect, with relatively small amplitude of their dispersion. In contrast, **after the transition ($g > g_c$)**, the gas fluctuations strongly localized near the domain wall—defect—in a gas (near kink at $\langle k_s \rangle$ site) and totally suppressed for anti-kink pinned by impurity site ($k = 0$). This localization is caused by the instability in the position k_s of the free-defect caused by the external noise. For the low-frequency noise, δg, the analytical estimation based on the linearized Langevin equations for δn_k gives a good agreement with numerical results obtained for nonlinear stochastic equation with multiplicative noise, see [1]. Note that similar fluctuation localization effect is also inherent for fluctuations induced by thermal reservoir for the long time scale.

In the end, note that similar effects can take place in the 2D- and 3D-cases for impurity clusters, that accompanied by the collective nonlinear dynamical screening effect [8,9].

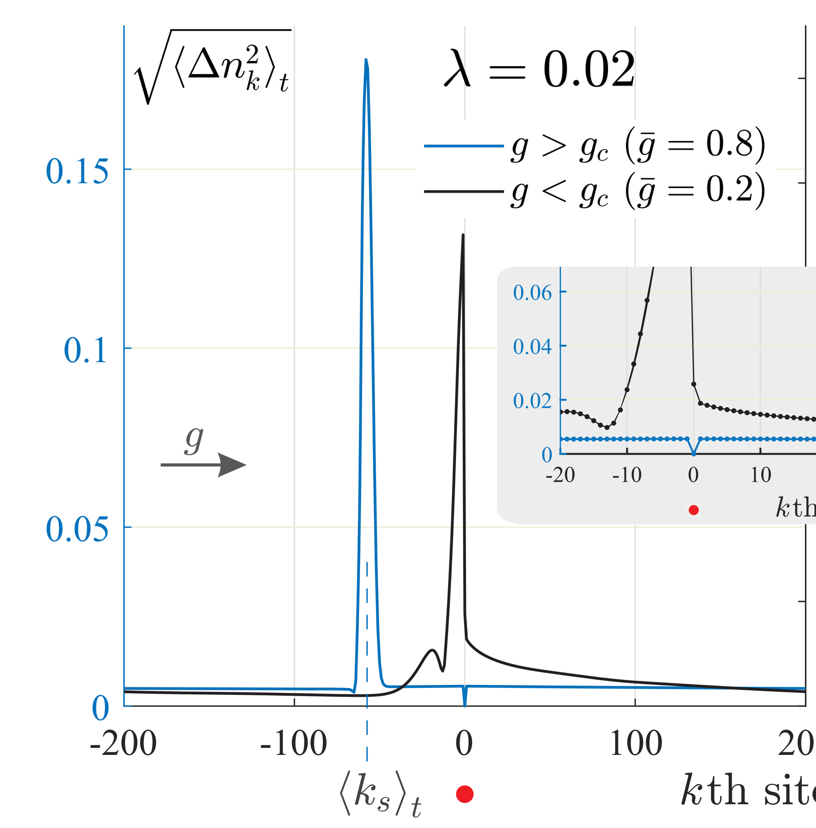

Figure 3: The square root dispersion $\langle \Delta n_k^2 \rangle_t^{1/2} = \langle (n_k - \langle n_k \rangle_t)^2 \rangle_t^{1/2}$ of the noise-induced fluctuations of the kth site occupation number for periodic random noise with $\lambda = 0.02$, below g_c ($\langle g \rangle_t = 0.2$) and above g_c ($\langle g \rangle_t = 0.8$). In the subcritical domain ($g < g_c$), the fluctuations induced by the multiplicative noise are mostly distributed near the impurity with the accumulation ahead of it, the site $k = 0$. On the contrary, in overcritical domain ($g > g_c$), the noise-induced fluctuations are totally suppressed in the impurity, $k = 0$, and strongly localized near the defect (the domain wall) position $\langle k_s \rangle_t$. This local enhancement of density-fluctuations intensity nearby the domain wall (phase coexistence layer) is caused by its back/forward trembling or, in other words, by noise-induced floating of the domain wall position with time. Inset shows the zoomed in region near the impurity, $k \in [-20\ 20]$. Other parameters: $2L = 400\ell$, $\bar{n} = 0.3$, and $U = 0.6$.

[1] S.P. Lukyanets, O.V. Kliushnichenko, *Nonequilibrium protection effect and spatial localization of noise-induced fluctuations: Quasi-one-dimensional driven lattice gas with partially penetrable obstacle*, Phys. Rev. E **109**, 054103 (2024)

[2] D.N. Zubarev, *Nonequilibrium Statistical Thermodynamics* (Plenum Press, New York, 1974).

[3] A.A. Tarasenko, P.M. Tomchuk, A.A. Chumak, *Fluctuations in the Bulk and on the Surface of Solids* (Naukova Dumka, Kyiv, 1992)

[4] A. Chumak, A. Tarasenko, *Diffusion and density fluctuations of atoms adsorbed on solid surfaces*, Surf. Sci. 91, 694 (1980)

[5] G. Bal, *Topological protection of perturbed edge states*, Commun. Math. Sci. **17**, 193 (2019)

[6] S. Yao, Z. Wang, *Edge states and topological invariants of non-hermitian systems*, Phys. Rev. Lett. **121**, 086803 (2018)

[7] V.M. Martinez Alvarez, J.E. Barrios Vargas, L.E.F. Foa Torres, *Non-Hermitian robust edge states in one dimension: Anomalous localization and eigenspace condensation at exceptional points*, Phys. Rev. B 97, 121401 (2018)

[8] O.V. Kliushnychenko, S.P. Lukyanets, *Effects of gas interparticle interaction on dissipative wake-mediated forces*, Phys. Rev. E 95, 012150 (2017)

[9] O.V. Kliushnychenko, S. P. Lukyanets, *Effects of collectively induced scattering of gas stream by impurity ensembles: Shock-wave enhancement and disorder-stimulated nonlinear screening*, Phys. Rev. E **98**, 020101(R) (2018)

[10] S.A. Janowski and J.L. Lebowitz, Phys. Rev. A **45**, 618 (1992).; Stat. Phys. **77**, 35 (1994)

[11] K. Mallick, *The exclusion process: A paradigm for non-equilibrium behaviour*, Physica A **418**, 17 (2015)

[12] P. Greulich and A. Schadschneider, *Single-bottleneck approximation for driven lattice gases with disorder and open boundary conditions*, J. Stat. Mech. 2008, P04009 (2008)

[13] I. Lobaskin, M.R. Evans, and K. Mallick, *Current fluctuations in a partially asymmetric simple exclusion process with a defect particle*, Phys. Rev. E **109**, 024127 (2024)

[14] S. Shankar, A. Souslov, M.J. Bowick, M.C. Marchetti, V. Vitelli, *Topological active matter*, Nat. Rev. Phys. **4**, 380 (2022)

[15] L. Garbe, Y. Minoguchi, J. Huber, P. Rabl, *The bosonic skin effect: Boundary condensation in asymmetric transport*, SciPost Phys. **16**, 029 (2024)

[16] P.C. Cao, Y. Li, Y.G. Peng, M. Qi, W.X. Huang, P.Q. Li, and X.F. Zhu, *Diffusive skin effect and topological heat funneling*, Commun. Phys. **4**, 230 (2021).

[17] K. Dasbiswas, K.K. Mandadapu, S. Vaikuntanathan, *Topological localization in out-of-equilibrium dissipative systems*, Proc. Natl. Acad. Sci. U.S.A. 115, E9031 (2018)

[18] L.E.F. Torres, *Perspective on topological states of non-Hermitian lattices*, J. Phys. Mater. 3, 014002 (2019)